IMPACT STRENGTH OF CRACKED STRUCTURAL MEMBER

I. Maekawa and K. Uda
Kanagawa Institute of Technology
1030 Shimo-Ogino, Atsugi, Kanagawa, Japan

ABSTRACT

Impact tension, bending and torsion experiments are performed using precracked strip and pipe specimens made of polymethyl methacrylate. The dynamic strain concentration factor, $K_{d,\varepsilon}$, is evaluated on the basis of the dynamic strain histories measured at the crack-tip and the smooth portion of each specimen in terms of the strain gauge method. The magnitude of $K_{d,\varepsilon}$ of the short specimen is larger than that of the long one except for the pipe in the case of impact bending. The similar influence of specimen length on the dynamic stress concentration factor $K_{d,\sigma}$ is evaluated by numerical analysis. When the dynamic stress concentration factor is evaluated for the incident stress wave without the influence of reflected waves, it is influenced by the crack-tip geometry. But, the crack-tip geometry dose not influence on the static stress concentration factor, $K_{s,c}$, which is evaluated in a small region at a crack-tip by a new method.

KEYWORDS

Strip, pipe, PMMA, crack, impact experiment, numerical analysis, stress concentration factor.

1. INTRODUCTION

Under a static load, the stress intensity factor is conveniently used to evaluate the integrity of a cracked structural member without regarding for the size effect, if the product of the stress applied and the square root of crack length is equal to that of model for an analogous geometry. However, according to our previous investigations, the fracture strength of a specimen subjected to an impact force showed size dependence, which is named as the mechanical size effect [1,2]. Therefore, it is considered that the investigation on the influence of the length on the impact fracture strength of cracked member is important to secure the safe design. However, no investigations of this type have been reported except for our previous papers[1,2]. Thus, this report intends to clarify the influence of specimen length on the impact fracture strength using cracked strip and pipe specimens made of polymethyl methacrylate (PMMA).

Numerical analyses were also performed to consider the experimental results. Since the influence of the reflected waves is included in these results. Then, the influence of the crack-tip geometry on the dynamic stress concentration factor was also considered without the influence of the reflected waves. Furthermore, it has been pointed out that macroscopic stress analysis for a structural member should be related to the microscopic consideration, taking into account the atomic-level mechanical condition, in order to clarify the fracture mechanism [3]. But, microscopic

investigations do not always consider the loading condition [4,5]. Then, the influence of the crack-tip geometry on the static stress concentration factor is also numerically analyzed by a new method, which enable us to consider the microscopic stress concentration at a crack-tip under a given macroscopic loading condition, and the results were compared with the results of the investigation on the dynamic stress concentration factor.

2. EXPERIMENTAL

2.1 Preparation of Specimens

Long and short strip and pipe specimens made of PMMA were prepared. The Young's modulus and the density of this material are 2.99GPa and $12 \times 10^2 kg/m^3$, respectively. The width and the thickness of strip specimens were 80 and 5mm, respectively. The crack length, which was introduced on one side of each strip using cutter and falling weight, was 10mm. The outer and inner diameters of pipe specimens were 30 and 25mm, respectively, and a partial circumferential precrack was introduced with the length of 16, 12 and 19mm for impact tension, bending and torsion experiments, respectively.

2.2 Experimental Method and the Results

Impact tension, bending and torsion experiments were performed by the falling weight method, as shown in Figs. 1(a) ~ (e). In the case of the impact bending experiment, the cracked side of the specimen was set as for the tensile side, as shown in Figs.1 (b) and (d). Dynamic strains were measured by strain gages cemented at the crack-tip and the smooth portion of every specimen. The distance between a crack-tip and the centerline of the strain gage was 0.5mm. In the case of impact torsion, strain gauges were cemented at the crack-tip and the smooth portion of pipe at an angle of 45° to the axis of pipe, respectively. Every crack extended obliquely to the axis of pipe by an impact torsion. Typical examples of strain history are shown in Figs.2(a) ~ (d).

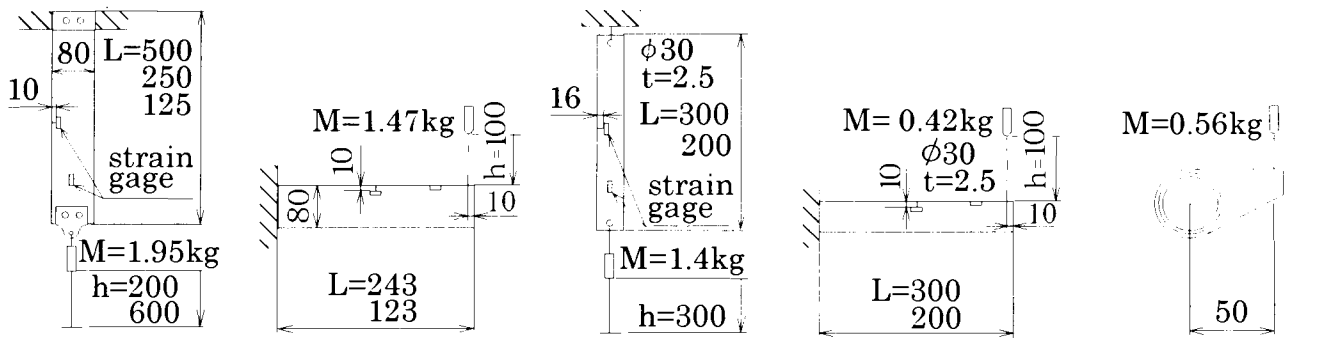

(a)Strip, tension (b)Strip, bending (c)Pipe, tension (d)Pipe, bending (e)Pipe,tortion (φ30,L=300,400)

Fig.1 Schematic illustrations of experiment.

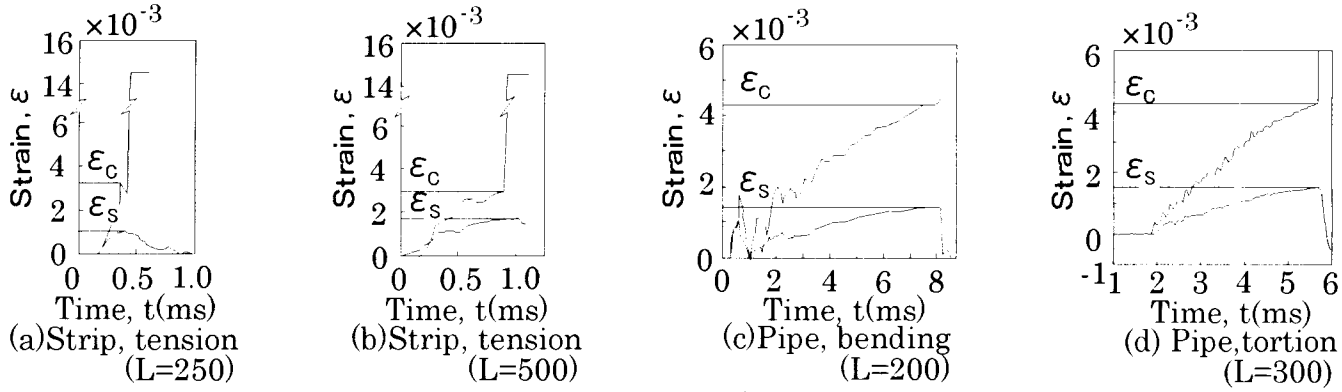

(a)Strip, tension (L=250) (b)Strip, tension (L=500) (c)Pipe, bending (L=200) (d) Pipe,tortion (L=300)

Fig.2 Typical examples of strain history.

Abrupt rise in strain is evident in each strain history measured at the crack-tip. This abrupt rise in strain was caused by the fracture of the strain gage due to the crack extension, and all specimens were fractured in a brittle manner. Thus, the strain, ε_c, at this point was considered to correspond to the impact fracture strength of the cracked specimen. On the other hand, no abrupt rise was observed in the strain history measured at the smooth portion of the specimen, but the maximum strain, ε_s, was observed at almost the same time as the time of the above mentioned abrupt rise in the strain history at the crack-tip. Next, the dynamic strain concentration factor was defined by $K_{d,\varepsilon} = \varepsilon_c / \varepsilon_s$. The influence of specimen length on $K_{d,\varepsilon}$ was shown in Fig.3.

In Fig.3, the magnitude of $K_{d,\varepsilon}$ of the short specimen is larger than that of the long one in all cases, except for the case of the impact bending of the pipe specimen. Comparing Figs.2 (a) and (b), it is evident that the magnitude of ε_c is almost the same, but that ε_s of the long specimen is slightly larger than that of the short one. The time, τ_c, to attain the fracture strain, ε_c, of the long specimen is also longer than that of the short specimen. This result implies that the stress amplitude was increased by the superposition of stress waves reflected at both ends of the specimen. However, in the case of impact bending, the magnitude of $K_{d,\varepsilon}$ of the short pipe specimen is little bit smaller than that of the long one, as shown above. In order to consider the reason for this, numerical analyses were performed by the finite element method (FEM) employing the DYNA3D.

3. NUMERICAL CONSIDERATIONS

3.1. *Influence of Specimen Length on the Dynamic Stress Concentration Factor*

The strip and pipe models were made of PMMA and divided into 400 and 600 elements, respectively. Typical examples of stress history are shown in Figs.4 (a) and (b). The stress wave propagates with the velocity, v, then, it needs the time $\tau_L = L/v$ to travel the specimen length, L. Since the time τ_L is shorter than the time τ_c to attain the maximum stress amplitude, σ_c, after the arrival of wave at the crack-tip, reflected waves were included in the maximum amplitude. Therefore, the dynamic stress concentration factor, $K_{d,\sigma}$, which was defined as the ratio of σ_c to σ_s at the smooth portion of model, was influenced by the length of model as shown in Fig. 5. Where, σ_s is the stress averaged for the time τ_c. Thus, the length dependences of $K_{d,\varepsilon}$ and $K_{d,\sigma}$ are also understood by considering the effect of superposition of mechanical waves, which means both strain and stress waves.

However, in the case of the pipe model, stress waves propagated in spirally between the outer and inner surfaces. Then, it is supposed that the dynamic stress distribution will be very complicated and different from other cases. This is the reason for the different length dependence. But, the computation needs very long time and so an exact analysis shall be performed in the future. In the case of impact torsion, the shearing stress showed very complicated history. And crack extended obliquely for the axis of pipe. Then, the fracture would be caused by the normal stress at the crack-tip. Therefore, the tensile stress component should be used rather than the shearing stress component in order to evaluate the dynamic stress concentration factor. However, the stress concentration factor for the tensile stress was considered in the case of impact tension as described above. Thus, stress history and the stress concentration factor are not described in the case of impact torsion.

3.2. *Influence of Crack-tip Geometry on the Dynamic Stress Concentration Factor*

As described above, reflected waves were included in the maximum amplitude, and the investigation for the microscopic region at a crack-tip is indispensable to clarify the fracture mechanism. Then, the influence of the crack-tip geometry on the dynamic stress concentration factor was numerically investigated for the incident wave without the influence of reflected waves. When an impact tension was imposed with the amplitude of 2MPa on the

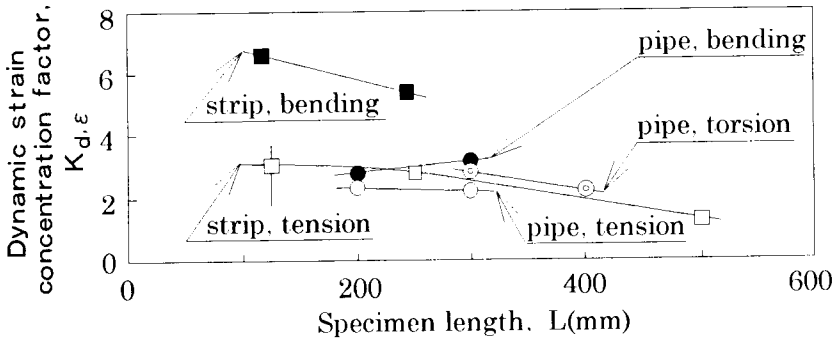

Fig.3 Influence of specimen length on $K_{d,\varepsilon}$.

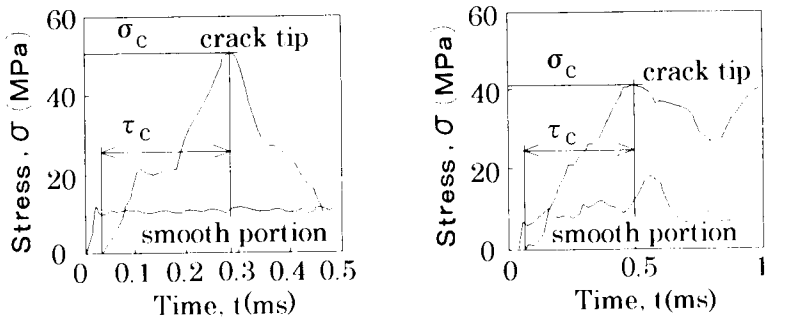

Fig.4 Examples of stress history.

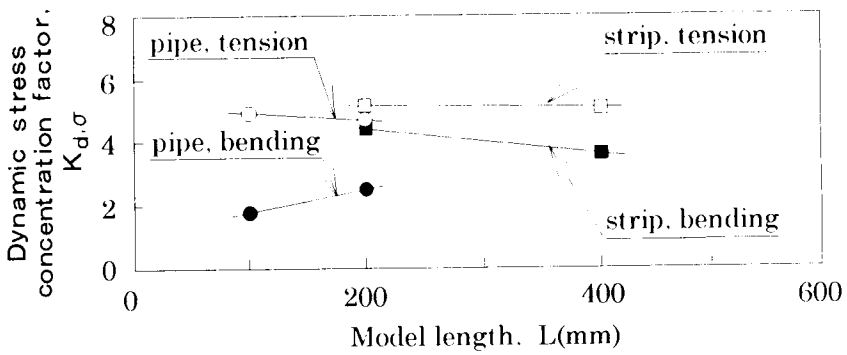

Fig.5 Influence of model length on $K_{d,\sigma}$.

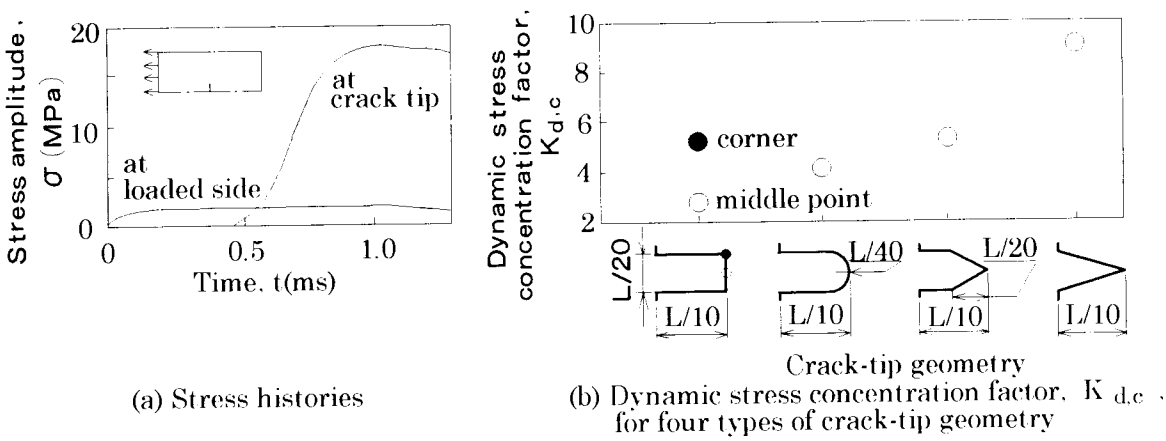

(a) Stress histories

(b) Dynamic stress concentration factor, $K_{d,c}$, for four types of crack-tip geometry

Fig.6 Dynamic stress concentration factor, $K_{d,c}$.

left side of the strip, which has a central crack, the stress histories were recorded at the loaded side and at the crack-tip as shown in Fig.6 (a). In this figure, the peak stress was recorded at the crack-tip. The dynamic stress intensity factor also shows similar peak [6]. In Fig.6 (a), no reflected waves came back to the crack-tip yet until the peak stress was attained. In this case, the dynamic stress concentration factor, $K_{d,c}$ was defined as the ratio of the peak stress to the stress amplitude of incident wave and shown in Fig.6 (b) for five types of crack-tip geometries. According to this figure, the magnitude of $K_{d,c}$ was influenced by the crack geometry.

3.3 *Influence of Crack-tip Geometry on the Static Stress Concentration Factor*

It is also important to determine how the dynamic stress concentration factor is different from static one. Thus, the influence of the crack-tip geometry on the static stress concentration factor was numerically investigated by a new

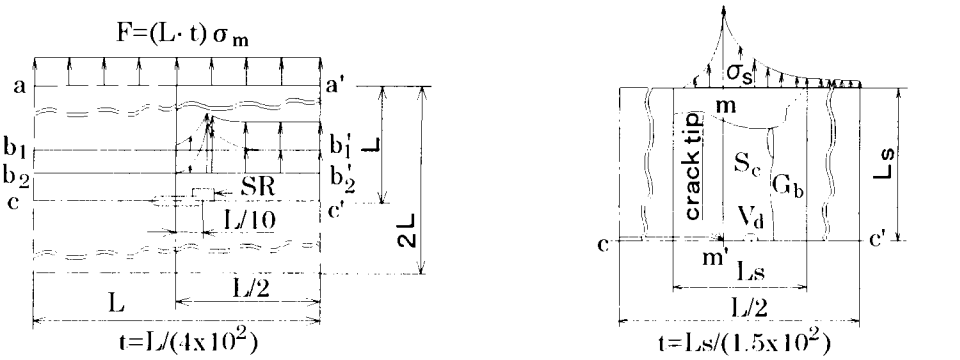

(a) Stress distribution in a (b) Magnified small regin, SR

Fig.7 Model of imaginary magnification method.

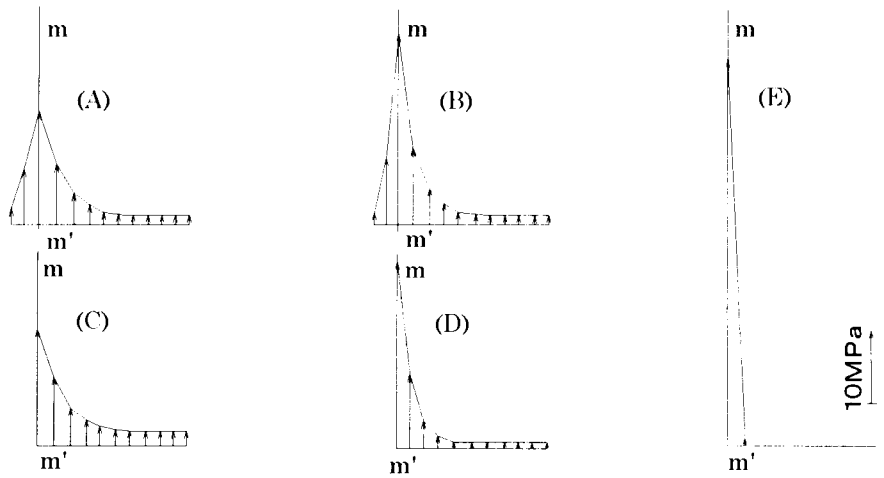

Fig. 8 Five types of the stress distribution on the upper side of magnified region.

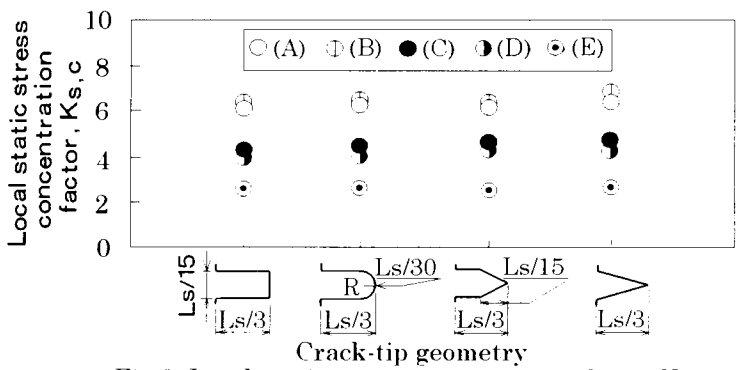

Fig.9 Local static stress concentration factor $K_{s,c}$ for four types of crack-tip geometry.

method. Usually, a crack is considered as a hairline crack. However, the geometry of a crack no longer resembles a hairline crack under the observation by a high magnification microscope [8]. It implies that it needs to change from engineering scale to microscopic one to investigate a microscopic geometry. Similarly, it is considered that the stress distribution in the microscopic region at a crack-tip should be analyzed using a microscopic scale, which is suitable to investigate the influence of microscopic geometry on the stress concentration at a crack-tip in detail, instead of engineering one as follows.

In the first step of this method, the stress distribution around a small region, SR, which includes a crack-tip, was analyzed for a strip with a central crack under a given tension, F. In the second step, the stress distribution was loaded on the boundary of the small region after an imaginary magnification, which is not merely a simple zooming up but also reveals small defects such as short crack, S_c, void, V_d, and grain boundary, G_b. These models are shown in Figs.7 (a) and (b). These models were divided into about 88 and 172 elements for the first and the second steps, respectively, and analyzed by FEM. Since the suitable magnification can not be predicted beforehand, five types of stress distributions are selected to simulate the stress distribution to be applied on the upper side of the small region as shown in Fig.8. The local static stress concentration factor was defined as $K_{s.c} = \sigma_c / \sigma_{m,L}$ in the small region, SR. Where, σ_c and $\sigma_{m,L}$ are the maximum stress at the crack-tip and the mean stress averaged over the length of upper side, L_s, of SR. The influence of crack-tip geometry on $K_{s.c}$ is shown in Fig.9. According to this figure, the crack-tip geometry does not influence on the magnitude of $K_{s.c}$.

4. CONCLUSION

Impact tension, bending and torsion experiments were performed using cracked strip and pipe specimens made of PMMA. Except for pipe specimen in the case of impact bending, the dynamic strain concentration factor of short specimen was slightly larger than that of long one. The similar influence of specimen length on the dynamic stress concentration factor is evaluated by numerical analysis. These size effects can be understood by considering the interference effect of mechanical waves. The dynamic stress concentration factor is also influenced by the crack-tip geometry, when it was evaluated without the influence of reflected waves. But the static stress concentration factor, which was evaluated in the microscopic region at a crack-tip by a new method, was not influenced by the crack-tip geometry.

ACKNOWLEDGEMENTS

The authors wish to express hearty thanks Mr. K. Inoue for his assistance in carrying out the experiments and Honda Metals co. for supplying materials. This work was partly supported by the Grant-in-Aid for Scientific Research of Japan Society for the Promotion of Science.

REFERENCES

1. Maekawa, I. (1997) Proc. of ICF9, Sydney, 6, 2743.
2. Maekawa, I. (1995) JSME Int. J. 38,80.
3. Yokobori, T. (1968) Int. J. Fact. Mech. 4,179.
4. Stroh, A.N. (1955) Proc. Roy. Soc. A232, 548.
5. Mullines, M.(1984)) Acta. Metall, 132, 381.
6. Itou, S. (1988) J. Appl. Mech. 47,801.
7. Bando, Y. (1984) J. Am. Ceram. Soc. C67, 36.